8/13/91
E 6020

# Dynamic Measurements of Gear Tooth Friction and Load

Brian Rebbechi, Fred B. Oswald, and Dennis P. Townsend
*Lewis Research Center*
*Cleveland, Ohio*

**NASA**

US ARMY
AVIATION
SYSTEMS COMMAND

# Dynamic Measurements of Gear Tooth Friction and Load

Brian Rebbechi[*], Fred B. Oswald, and
Dennis P. Townsend
National Aeronautics and Space
Administration
Lewis Research Center
Cleveland, Ohio 44135

## 1. INTRODUCTION

The dynamic forces at the point of tooth contact are of considerable interest to the designers of high-speed, light-weight gearing. Accurate prediction of the dynamic loads can assist in minimizing the size and weight of a transmission. In a helicopter application, where the transmission is a significant fraction of vehicle weight, such a reduction would be an important factor in overall vehicle performance.

A program to experimentally and theoretically study fundamental mechanisms of gear dynamic behavior is being undertaken at the NASA Lewis Research Center in support of a joint research program between NASA and the U.S. Army. This paper presents the results of dynamic tooth-fillet strain gage measurements from the NASA gear-noise rig, and it introduces a technique for using these measurements to separate the normal and tangential (friction) components of the load at the tooth contact. Resolution of the contact force is desirable for several reasons. Two of these reasons are the following:

(1) A primary output of analytical models of gear dynamic behavior is typically the normal force at the point of contact (e.g., [1] and [2]).

(2) The measurement of dynamic friction of meshing gears does not appear to have yet been carried out successfully. An interesting trial was carried out by Benedict and Kelly [3], but it was discontinued because of dynamic response

problems. Anderson and Lowenthal [4] computed overall losses due to friction and found good agreement between theoretical predictions and experimental data. Krantz and Handschuh [5] applied a similar technique to an epicyclic gear rig, obtaining good correlation at low oil temperatures, but poorer correlation at higher oil temperatures. However, this technique cannot detect the variation in friction during the tooth engagement cycle. There is also the problem of separating the power loss due to gear tooth friction from power losses due to other sources such as bearings, windage, and so forth.

Extensive measurements of lubrication conditions at a sliding-rolling contact have been carried out on disk machines [6]. These experiments are of considerable value in confirming the existence of elastohydrodynamic lubrication and in identifying the separate regimes of lubrication that prevail under the various slide-to-roll ratios. However, the usefulness of the modes of behavior and friction coefficients in predicting lubrication conditions at an actual tooth contact, where the degree of sliding changes throughout the tooth engagement cycle (typical duration, 250 $\mu$sec), needs to be verified. In this short period of time, large changes occur in the lubricant temperature, shear, and viscosity at pressures up to 1.4 GPa (200 000 lbf-in.$^2$). Dyson [7] reported temperatures up to 400 °C and oscillatory shear rates up to $10^7$ sec$^{-1}$. These conditions cannot readily be produced outside of an actual tooth mesh.

[*]Visiting scientist from Australian Aeronautical Research Laboratory.

Friction at the tooth contact is important for determining not only power loss and efficiency, but also for understanding gear-tooth scoring and wear. An important parameter in scoring is the friction coefficient [3]. Friction greatly affects the heat input to the lubricant when sliding velocities are high.

This report presents dynamic, gear-tooth strain measurements from low-contact-ratio spur gears tested in the NASA gear-noise rig. The technique used to convert these strain measurements into normal and tangential (friction) tooth loads is described. Plots of normal and tangential forces, for both static and dynamic conditions, are presented for a representative range of loads and speeds. The normal force and dynamic strain data have been used to verify a gear dynamics code in another related report [8].

## 2. APPARATUS

### 2.1 Test Facility

These tests were conducted in the NASA Lewis gear-noise rig (Fig. 1). This rig comprises a simple gearbox powered by a 150-kW (200-hp) variable speed electric motor, with an eddy-current dynamometer that loads the output shaft. The gearbox can be operated at speeds up to 6000 rpm. The rig was built to carry out fundamental studies of gear noise and of dynamic behavior of gear systems. It was designed to allow testing of various configurations of gears, bearings, dampers, and supports.

A poly-V belt drive served as a speed increaser between the motor and input shaft. A soft coupling was installed on the input shaft to reduce input torque fluctuations caused by a nonuniformity of the belt at the splice.

Test gear parameters are shown in Table 1, test rig parameters in Table 2, and gear tooth profile traces in Fig. 2. The tooth surface roughness was measured by using an involute-gear-checking machine with a diamond stylus of approximately 10-$\mu$m (0.0003-in.) radius. The surface roughness varied along the length of the tooth, with the region near the root appearing to be lightly polished. The maximum surface roughness was estimated to be 1.34 $\mu$m (34 $\mu$in.) peak-to-peak, or an average of 0.43 $\mu$m (11 $\mu$in.) (Fig. 3). The gear rig was operated at an oil fling-off temperature of 54±2 °C (130±5 °F). At the mean temperature of 54 °C, the viscosity of the synthetic oil (Table 2) used in the tests was 14 cSt (11.6 cP). Natural frequencies from a four degrees-of-freedom eigensolution [8] are also shown in Table 2.

### 2.2 Instrumentation

General-purpose, constantan foil, resistance strain gages (gage length, 0.38 mm (0.015 in.)) were installed in the tooth-root fillets on both the loaded (tensile) and unloaded (compression) side of two adjacent teeth on the output (driven) gear (Fig. 4). To measure maximum tooth bending stress, the gages were placed at the 30° tangency location [9].

Strain gage signals were conditioned by two methods: for static calibration and measurement, a strain gage (Wheatstone) bridge was used; for dynamic measurements, the strain gages were connected via a slip-ring assembly to a set of constant-current strain gage amplifiers.

A 4-channel, 14-bit digital data acquisition system was used to record the dynamic strain data. Sample rates of 20 to 50 kHz per channel were used, depending on test gear speed.

An optical encoder was mounted on the input shaft to measure roll angle and hence determine load location; the position of the encoder was adjusted so it would produce 1 pulse/revolution at a known roll angle.

## 3. TEST PROCEDURE

### 3.1 Calibration

Calibration of the strain gages on the instrumented (driven) gear was conducted to provide a matrix of strain output versus applied load. Before commencing the strain gage calibration, the gears were demagnetized. This demagnetization reduced the apparent strain resulting from the gages moving through the magnetic field of the adjacent gear. At normal gear operating speeds, magnetic effects can induce an error signal in the gage.

For calibration, the instrumented gear was meshed with a special gear whose adjacent teeth had been ground away; this permitted loading of a single tooth only. The calibration was carried out for each of the two instrumented teeth for roll angles ranging from 12° to 30°. At each test position (roll angle) the torque was applied at three levels – 45 percent, 88.5 percent, and 132 percent of the nominal value of 71.8 N-m (635 in.-lb). At each of these load levels the sliding direction was reversed (by reversing roll direction), and a linear curve was fit to the data for each sliding direction. By reversing the roll direction, the instrumented gear was effectively tested as both the driven gear (output) and driving gear (input). In each instance the gear was rotated a small angle (approximately 1°) in the intended direction of roll until the desired roll angle was reached, so as to definitely establish a sliding direction.

The strain gage calibration apparatus is shown in Fig 5. The results of the calibration for gages 1 to 4 are given in Figs. 6 and 7, for loading on tooth 1. The arrows indicate roll direction. The results for loading on tooth 2 were very similar.

2
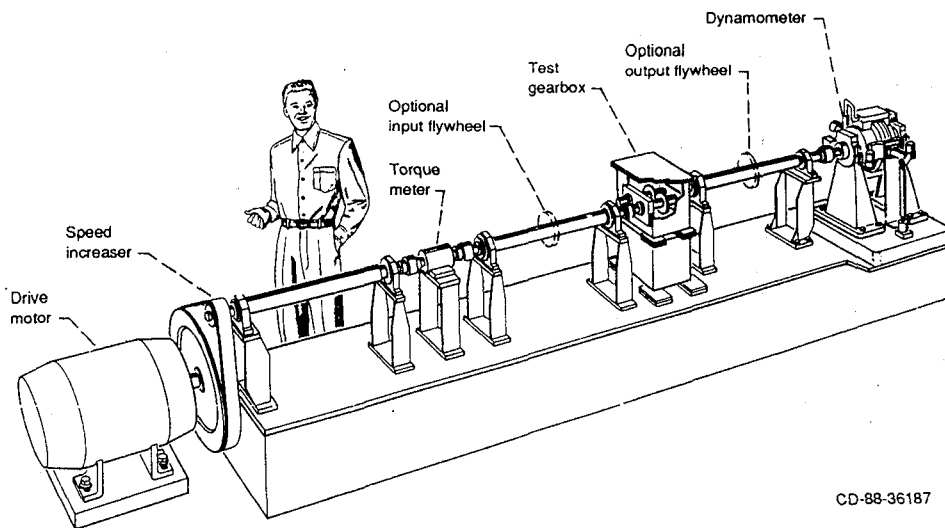
(a) Layout.

CD-88-36187
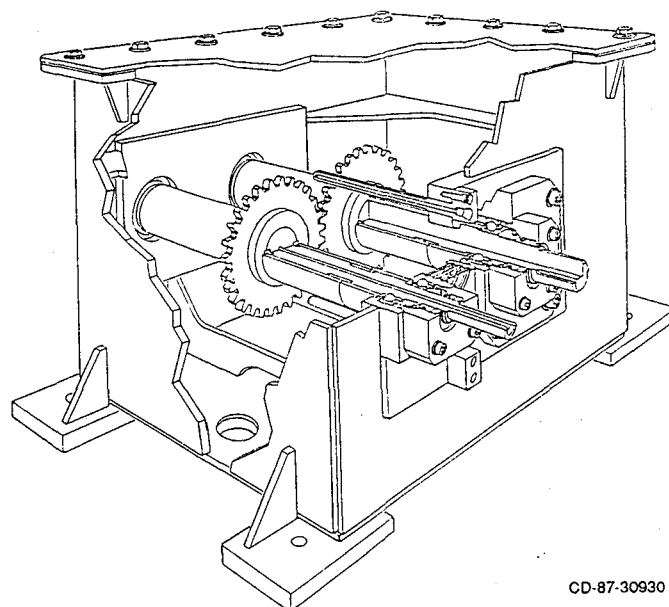


CD-87-30930

(b) Detail of gearbox.

Figure 1.—NASA gear-noise rig.

TABLE 1. – TEST GEAR PARAMETERS

| | |
|---|---|
| Gear type . . . . . . . . . | standard involute, full-depth tooth |
| Number of teeth . . . . . . . . . . . . . . . . . . . . . . . . . . . | 28 |
| Module, mm (diametrial pitch in.$^{-1}$) . . . . . . . . . | 3.175(8) |
| Face width, mm (in.) . . . . . . . . . . . . . . . . . | 6.35 (0.25) |
| Pressure angle, deg . . . . . . . . . . . . . . . . . . . | 20 |
| Nominal (100-percent) torque, N-m (in.-lb) . . | 71.77 (635.25) |
| Theoretical contact ratio . . . . . . . . . . . . . . . . | 1.64 |
| Driver modification amount, mm (in.) . . . . . . | 0.023 (0.0009) |
| Driven modification amount, mm (in.) . . . . . . | 0.025 (0.0010) |
| Driver modification start, deg . . . . . . . . . . . . . | 24 |
| Driven modification start, deg . . . . . . . . . . . . . | 24 |
| Tooth root radius, mm (in.) . . . . . . . . . . . . . | 1.35(0.053) |
| Average surface roughness, $\mu$m ($\mu$in.) . . . . . . . . | 0.43(11) |

3

TABLE II. - TEST RIG PARAMETERS

```
Input inertia, J₁, kg-m² (lb-sec²-in.) . . . . . . 0.0237 (2.10)
Gear inertia, J₂, J₃, kg-m² (lb-sec²-in.) . 0.0000364 (0.00322)
Load inertia, J₄, kg-m² (lb-sec²-in.) . . . . . . . 0.085 (7.5)
Input stiffness, K₁, N-m/rad (lb-in./rad) . . . . 341 (3017)
Gearbox stiffness, K₂, N-m/rad (lb-in./rad) . . . 6158 (54 500)
Load stiffness, K₃, N-m/rad (lb-in./rad) . . 12 700 (112 300)
Synthetic turbine oil . . . . . . . . . . . . . MIL-L-23699B
    Viscosity at 130 °C, cSt, (cP) . . . . . . . . . 14 (11.6)
Natural frequencies (eigensolution), Hz . . 6.56, 52.5, 1220
```
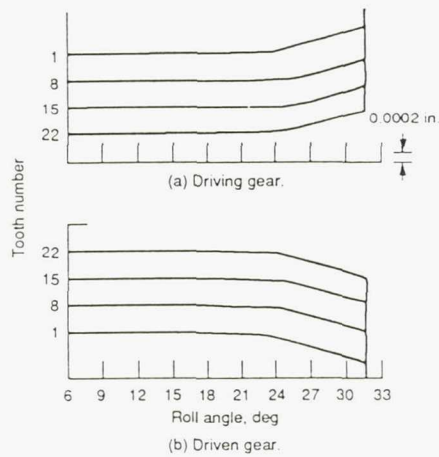


Figure 2.—Test gear profile traces.

(a) Driving gear.
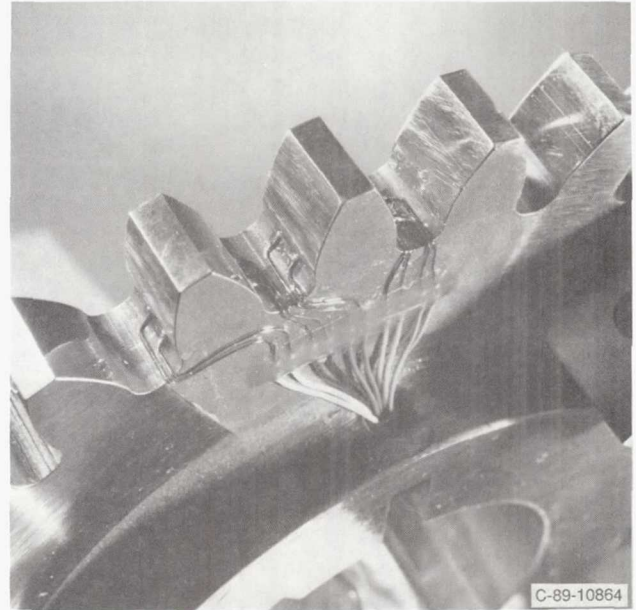
(b) Driven gear.
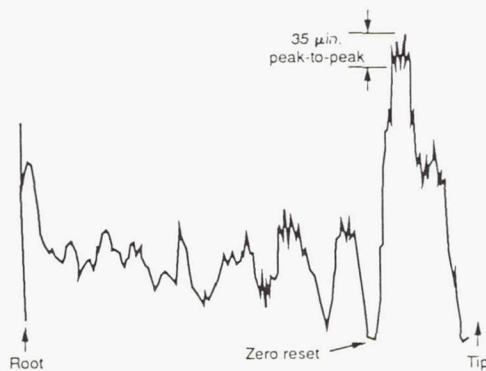


(a) Gage installation.



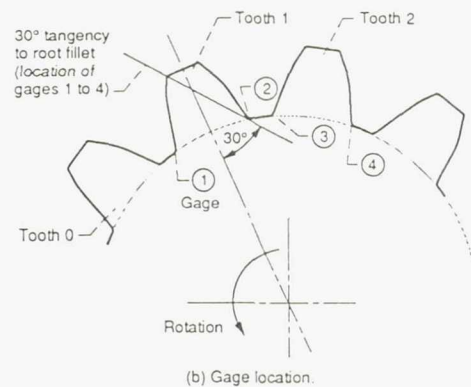Figure 3.—Surface roughness measurements of driven gear.



(b) Gage location.

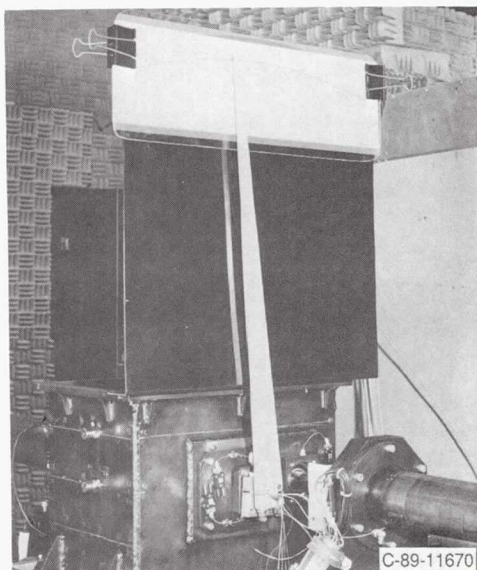Figure 4.—Strain gage installation and location on test gear.
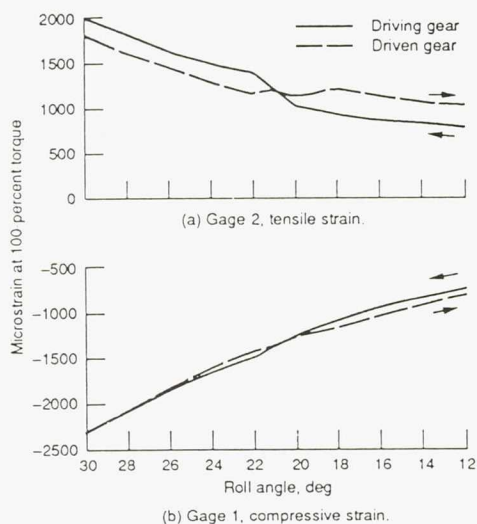
4

Figure 5.—Strain gage calibration apparatus.



(a) Gage 2, tensile strain.

(b) Gage 1, compressive strain.

Figure 6.—Static strain gage data, single tooth loading on tooth 1 (arrows show roll direction).



(a) Gage 4, tensile strain.
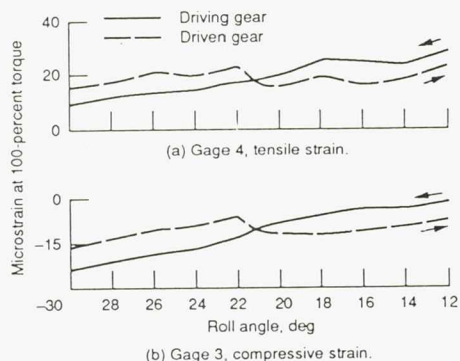
(b) Gage 3, compressive strain.

Figure 7.—Static strain gage data measured at tooth 2 for single-tooth loading on tooth 1 (arrows show roll direction).

## 3.2  Data Acquisition

3.2.1  Static strain data. – Strain data were recorded under static (nonrotating) conditions for the gear set assembled in its normal (running) configuration with the standard running gear replacing the calibration gear. The measurements were made for two reasons: first, as a check on the accuracy of the method used to resolve tooth force into normal and tangential components; and second, to provide information on load sharing characteristics of the gear assembly. A strain gage bridge circuit was used to record strains for roll angles from 12° to 40° relative to tooth 2. Torque levels of 37, 88, 100, and 132 percent were applied, but unlike the single-tooth case, linear curve-fitting of these data was not appropriate because of the kinematic non-linearities introduced by load sharing when more than one pair of teeth are in contact. As for the single-tooth case, these measurements were carried out for the instrumented gear acting as both the driven and driving gear, thus reversing the sliding direction.

3.2.2  Dynamic strain data. – Dynamic strains were recorded for the 4 gages, for a speed-load matrix of 28 points: 4 speeds (800, 2000, 4000, and 6000 rpm) and 7 torque levels (16, 31, 47, 63, 79, 94, and 110 percent of the nominal value of 71.8 N-m (635 in.-lb)). The data were recorded by 14-bit data recorders via a slip-ring assembly. Sample rates used were 50 000 Hz per channel for the 2000-, 4000-, and 6000-rpm speeds, and 20 000 Hz per channel for the 800-rpm speed. A continuous record, consisting of 10 000 data scans, was made at each speed so as to give a record length of 0.2 sec at 50 000 Hz, and 0.5 sec at 20 000 Hz. Because of the interest in comparing tensile and compressive strains on each tooth, data from these two gages were simultaneously recorded along with the encoder signal. This procedure was repeated for the second instrumented tooth.

The data were then digitally resampled, by using linear interpolation, at either 1000 or 2000 samples per revolution (depending on speed) and synchronously averaged. Time domain synchronous averaging, a technique now in wide use in gear diagnostics [10], was used here to reduce noise effects (especially from the torque fluctuation caused by the belt drive). Its implementation requires two data channels – one for timing signal data and one for strain data. The timing signal data provided resample intervals for exactly one revolution.

## 4.  ANALYSIS

For a single tooth, measurement of the strain outputs $S_c$ and $S_t$ of gages mounted on the compressive and tensile sides of the tooth respectively (Fig. 4) will, in principle, enable resolution of the tooth forces $F_n$ (normal) and $F_f$

(tangential), provided that the response of these two gages to the two forces is linearly independent. The response of the gages can then be expressed as

$$S_c = a_{11}F_n + a_{12}F_f \qquad (4.1)$$

$$S_t = a_{21}F_n + a_{22}F_f \qquad (4.2)$$

or simply as

$$\{S\} = [a]\{F\} \qquad (4.3)$$

where $\{S\} = \begin{Bmatrix} S_c \\ S_t \end{Bmatrix}$

$$\{F\} = \begin{Bmatrix} F_n \\ F_f \end{Bmatrix}$$

and $a_{ij}$ is the strain influence coefficient; that is, the strain at i due to a unit normal force (j = 1) or a unit friction force (j = 2).

The strain influence coefficients $a_{ij}$ are evaluated by alternately setting $F_n$ and $F_f$ in equations (4.1) and (4.2) to zero. In practice, neither $F_n$ nor $F_f$ can actually be zero because a normal force between the teeth is a prerequisite for a sliding force to develop. However, because strain values were recorded for both directions of sliding (that is, for the instrumented gear acting as both driving and driven gear) at each roll angle value, we inferred that the average of these two strain values is equivalent to the frictionless case, and that the effect of friction alone will be one-half the difference between the two values. Thus, the coefficients $a_{12}$ and $a_{22}$ (which relate to friction) are evaluated from half the difference between the driving gear and driven gear curves of Fig. 6. Likewise, the strain coefficients $a_{11}$ and $a_{21}$ (which relate to normal force) are evaluated from the average of these two curves. The solution for $F_n$ and $F_f$ is found by premultiplying both sides of equation (4.3) by $[a]^{-1}$; hence

$$\{F\} = [a]^{-1}\{S\} \qquad (4.4)$$

The analysis presented above ignores the influence on strains $S_c$ and $S_t$ due to loading on adjacent teeth. In the case of thin-rim gears [11], this effect can be on the order of 12 percent. For the thick-rim gears used here, however, the influence from adjacent teeth is at most 3 percent (compare Figs. 6 and 7). In the data presented in this paper, the influence of adjoining teeth has been included. The computational procedure is outlined in the Appendix.

## 5. RESULTS AND DISCUSSION

### 5.1 Calibration

Tooth-fillet strains for 100-percent torque were evaluated by fitting a linear curve to the calibration data for the three torque levels. These strains at gages 1 to 4 are plotted in Figs. 6 and 7 as a function of roll angle, for loading of tooth 1. Notable from these curves is the significant influence of static friction on strain output; the tensile gage (see Fig. 6(a)) shows a difference in strain between the driving- and driven-gear cases (when sliding direction reverses) that is 27 percent of the mean strain reading. The significance of this is twofold: first, it is difficult to establish a "no-friction" curve; and second, and possibly more important, these curves (particularly the tensile curve) illustrate the effect that tooth friction has on the results. It is apparent from Fig. 6 that the compressive gage is much less influenced by friction and, thus, would be expected to give the best indication of normal force if only one gage were used. This is further confirmed by the tooth strain influence coefficients (see Appendix).

### 5.2 Static Meshing

Measured strain is plotted in Fig. 8 as a function of roll angle for static meshing of the gears (i.e., for multiple-tooth contact). This figure shows the average strain (mean of driving- and driven-gear values) for 37-, 88-, 100-, and 132-percent torque. Figure 9 shows in greater detail the tooth-fillet strains for
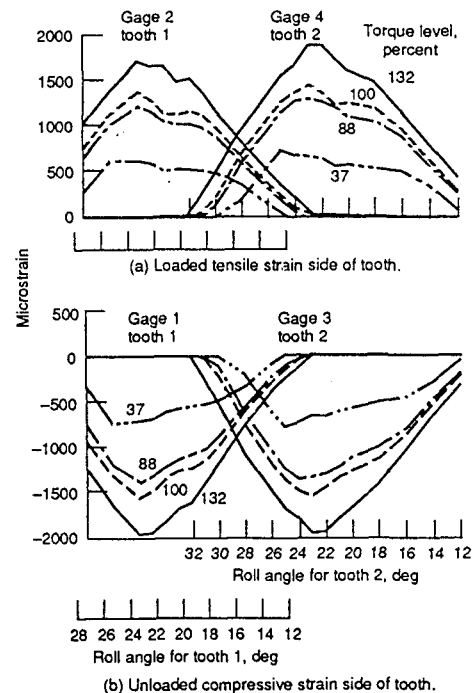


Figure 8.—Averaged static strain data on two successive teeth.

6

gages 1 to 4 at 100-percent torque, with the instrumented gear acting as both driven and driving gear. The curves of Fig. 9 are the averaged result of three trials. From the results of Fig. 9, and the influence coefficient matrix previously described, plots of normal and friction forces (Fig. 10) have been derived from the static data for the 100-percent-torque case.
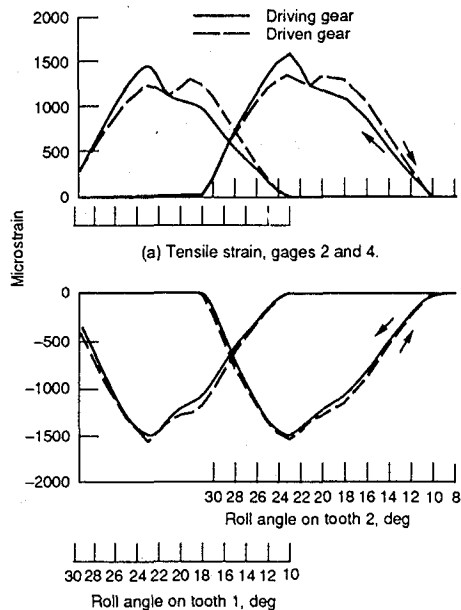


(a) Tensile strain, gages 2 and 4.

Roll angle on tooth 2, deg

Roll angle on tooth 1, deg

(b) Compressive strain, gages 1 and 3.

Figure 9.—Static strain data, multiple tooth loading (arrows show roll direction).



(a) Driving gear.

Roll angle on tooth 1, deg

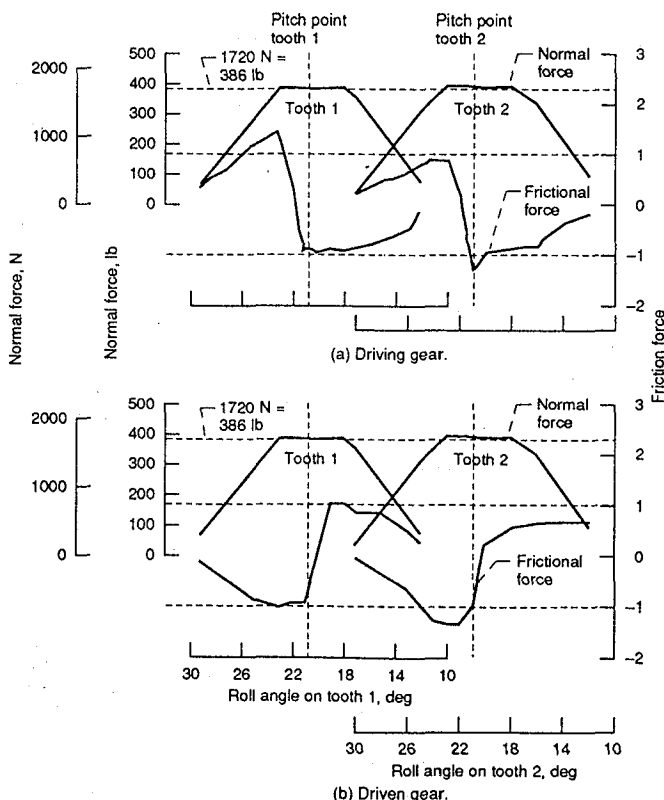Roll angle on tooth 2, deg

(b) Driven gear.

Figure 10.—Normal and frictional forces at 100-percent torque under static conditions.

The total normal force between the one- or two-tooth pairs in mesh should be equal to 1718 N (386 lbf). This value is the torque divided by the base circle radius. The normal-force component of the plots shows agreement within 1.5 percent of the expected value.

An absolute value for the friction force cannot be determined during calibration since the coefficient of friction at the tooth contact point is unknown. If an arbitrary value of unity is assigned to the maximum frictional force developed at 100-percent torque, then the friction value should be either +1 or -1 (depending on the direction of sliding) in the single-tooth contact region. This ideal is nearly achieved in the static measurements for tooth 1 in Fig. 10(b). For tooth 2, the friction force is offset by about -0.4 from the +1 values. Outside the single-tooth contact region, the friction force decreases in approximately linear fashion with the normal tooth load. This implies a constant friction coefficient under these static meshing conditions.

It is interesting to note the location of the zero-crossing of the friction force in Fig. 10 when tooth sliding changes direction. This zero-crossing differs from the pitch point by nearly 1° of roll. Some of this difference may be due to deflection of the gear shaft, which causes a shift in the operating pitch point.

5.3 Dynamic Case

The dynamic tooth strains for the 28 speed-load conditions are shown in Fig. 11. To allow direct comparison, the compressive strain data are inverted (shown as positive) and overlayed on the tensile curves. Notable features of these curves include the peak tooth strain corresponding with the high point of single-tooth contact (which occurs at about 23° roll angle), a dip or notch in the tensile tooth strain curves near the pitch point (where the sliding force reverses), and dynamic effects becoming apparent at higher speeds.

The dynamic effect is particularly notable in the curves for 4000 rpm at the lowest torque (16 percent). Here, the force vanishes, thereby indicating tooth separation occurs. By contrast, at 110-percent torque there is very little dynamic effect, as evidenced by little difference among the curves for the four speeds (800, 2000, 4000, and 6000 rpm).

In Fig. 12 the computed normal and friction forces are shown for four speeds at the highest torque (110 percent). Note the very good agreement with expected results at the low speed of 800 rpm (Fig. 12(a)), where we would expect to approach a static case. Here, the normal force is very close to the static nominal value (a function of the torque divided by the base circle radius). The friction results show a marked transition in force from negative to positive as the tooth contact passes through the pitch point, where

7

there is pure rolling. Also the friction
coefficient appears to be less than that of
the static calibration case, as can be seen
by comparing Fig. 10(a), where the friction
force has a value of unity for a normal
force of 386 lbf, and Fig. 12(a), where the
friction force is a maximum of approxi-
mately ±0.75.

## 5.4 Accuracy

The results obtained herein for the
static and dynamic tests indicate the
feasibility of using multiple gages to
separate the tooth friction and normal
forces. The results of the static case are
particularly encouraging. The value for
the normal force is generally within
1.5 percent of the expected value. The
friction force, whilst at times much less
accurate, nonetheless demonstrates the
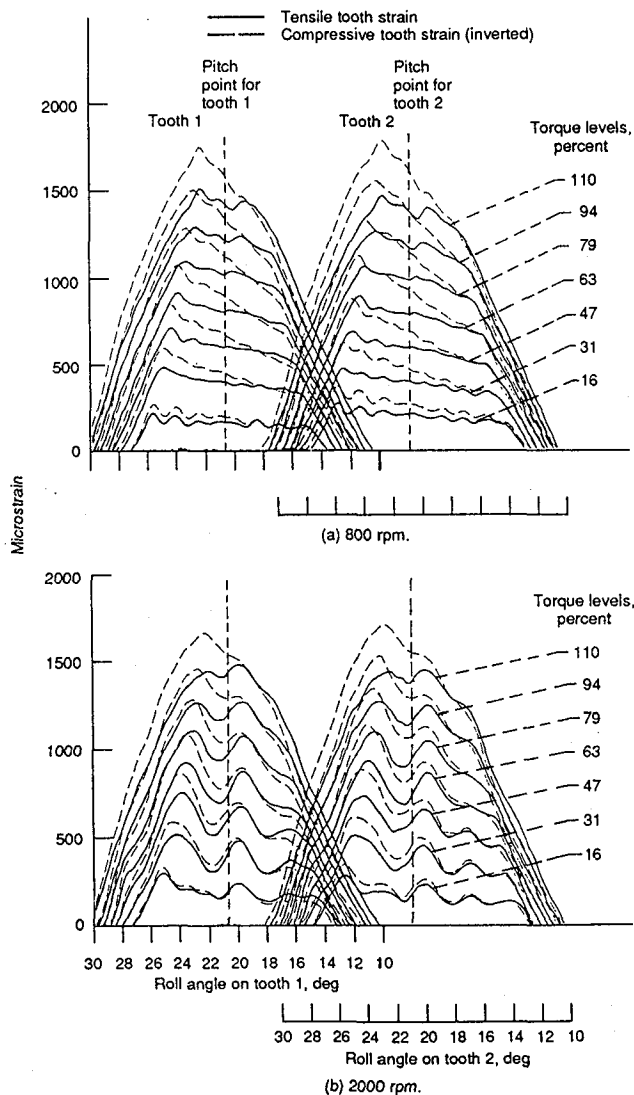trends we expected to see – that is, the



(a) 800 rpm.

(b) 2000 rpm.

Figure 11.—Dynamic tooth strains at four speeds and seven torque levels.
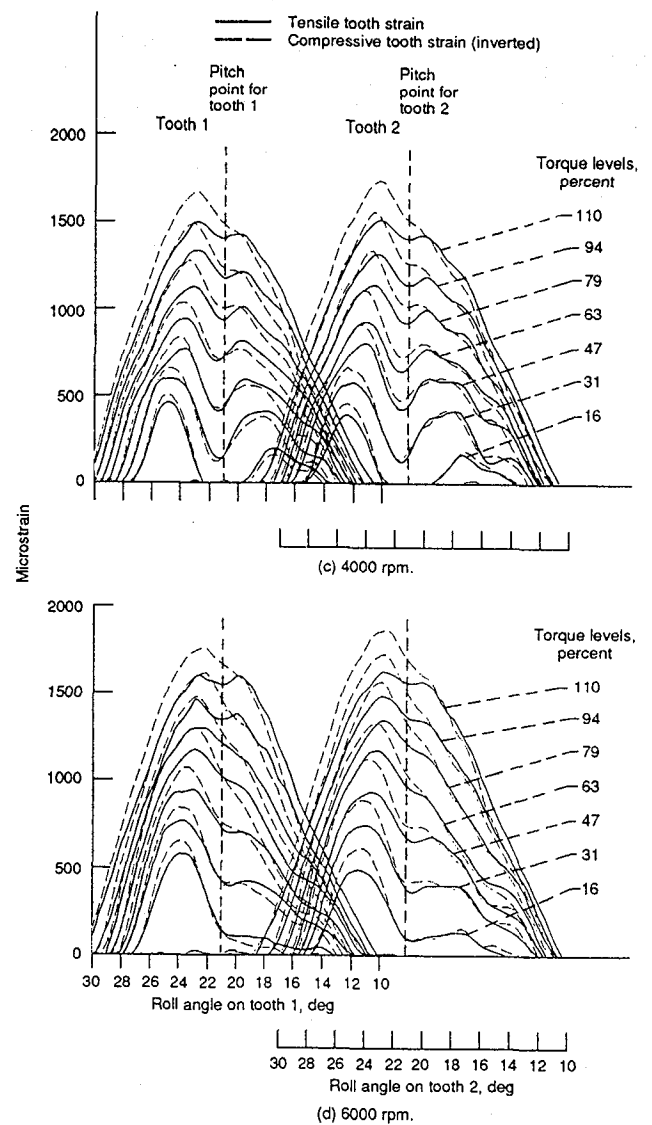Compressive strains are shown as positive for comparison with tensile
data.



(c) 4000 rpm.

(d) 6000 rpm.

Figure 11.—Concluded.

friction force is proportional to the nor-
mal load, and a reversal in sign occurs at
about the pitch point. The good results
for the static case are believed to be
partly due to using instrumentation that
was identical to that used for the static
calibration (i.e., the Wheatstone bridge
circuit). Assessing the accuracy for the
dynamic case is more difficult, since we do
not fully know what to expect. However,
dynamic operation could introduce the fol-
lowing problems:

(1) There could be some change in sen-
sitivity due to the change in signal condi-
tioners (i.e., constant current amplifiers
operating through slip rings).

(2) Resistance variations of the slip
rings and other electrical noise can con-
taminate dynamic data. This was minimized
here by the use of synchronous averaging,
as described in the test procedure for
dynamic data.

(3) Other dynamic effects such as gear
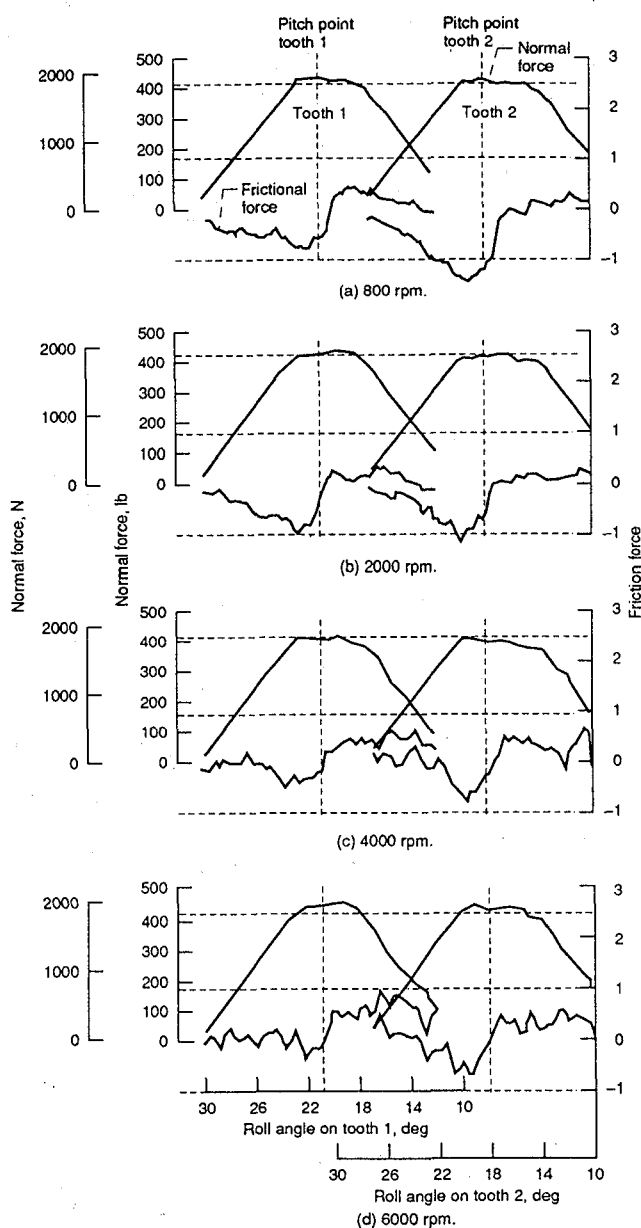body vibration can also produce unwanted

8

Figure 12.—Computed dynamic load and friction at four speeds and 110-percent torque.



Figure 13.—Computed dynamic load and friction superimposed for four successive revolutions at 4000 rpm and 110-percent torque.

the summing of the strain magnitudes, as is the case for normal force (see Appendix). Various techniques can be used to minimize errors – synchronous averaging, as carried out here, and possibly, an adjustment (compensation) of the friction curve to bring about zero friction at the pitch point. The dc offset of the strain signal is critical. Figure 13 shows the superimposed curves of normal and friction forces for four successive revolutions of the gear, using nonaveraged data. Each curve is based on the corresponding tensile and compressive strains for that particular revolution. A significant variation in friction estimation is evident from one revolution to the next; this cannot be ascribed to the expected small torque fluctuations caused by the belt drive.
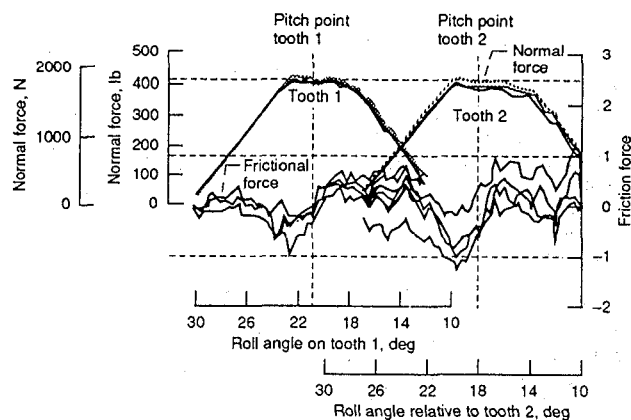
signals. A strain output from the tooth fillet gages was observed when the teeth were out of mesh. This is attributed to vibration of the gear body. The effect was most obvious at higher speeds, appearing at three times tooth mesh frequency. This frequency component can be seen in the friction force trace at 6000 rpm (Fig. 12(d)).

Using strain outputs to detect friction requires accurate measurement of strain. A 1-percent error in strain measurement will result in a 10-percent error in force estimation (see Appendix). This extreme sensivity to measurement error occurs only with friction force estimation. It effectively results from using the difference between the magnitude of the tensile and compressive strains, rather than

Differences in profile between the single-tooth calibration gear and the operating gear result in the tooth contact point being slightly displaced along the tooth profile, thereby causing an error in the measured roll angle. This error has been estimated to be of the same order (0.25°) as the error in setting the roll angle for calibration.

The friction force results obtained herein were necessarily qualitative. A logical next step would be to calibrate the gages with a known friction force. A device similar to that of Benedict and Kelly [3] (Fig. 14) could be used for this purpose. In their application, dynamic effects prevented Benedict and Kelly from obtaining useful results from this device. If the device were used only for static calibration, this restriction would be removed. Alternatively, with only slight modification this setup could be used to apply a known force in the friction force direction while the tooth contact position was held constant.
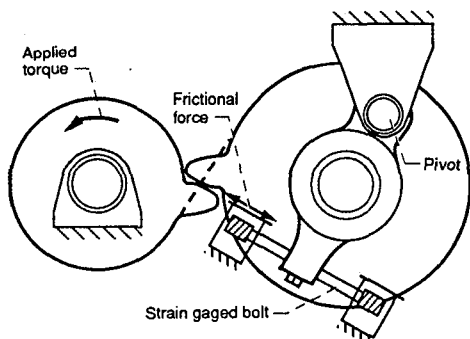
Figure 14—Gear friction measurement apparatus, modified from Benedict and Kelley (1961).

## 6. SUMMARY OF RESULTS

Tooth-fillet strains were recorded for 28 operating conditions on the NASA gear-noise rig. A method was introduced that used the tensile and compressive tooth-fillet strains to transform these strain measurements into the normal and frictional loads on the tooth. This technique was applied to both the static and dynamic strain data. The results demonstrated that this technique was viable, and in particular they showed the following:

1. For the static case, the normal force closely agreeed (within 1.5 percent) with expected results. The frictional results were much more variable, but they exhibited expected trends.

2. In the dynamic case, the estimation of normal force was good, the friction results, less so. However, the friction force results showed expected trends; that is, the dynamic friction coefficient was less than the static coefficient, and the friction reversed direction near the pitch point. Further refinement of measurement techniques will be required to produce more accurate results.

3. The influence of sliding friction was particularly marked on the tension tooth-fillet gage. The compression gage was affected by friction to a much lesser degree.

## APPENDIX

### TOOTH FORCE INFLUENCE COEFFICIENT MATRIX

The meshing cycle of a tooth on a low-contact-ratio spur gear may be divided into 3 cases: (1) the tooth load is shared with the preceeding tooth; (2) the entire load is carried by the tooth; and (3) the load is shared with the following tooth. We have shown earlier that loading on the adjacent (preceeding or following) tooth will produce a small influence on a tooth-fillet strain gage.

The normal and frictional components of force on a gear tooth may be computed from equation (4.4), expanded to a six-by-six matrix. To compute the forces on tooth 1, we must know the output of strain gages on the adjacent teeth (designated 0 and 2) due to loading on tooth 1. Although we did

not measure the strain on tooth 0, we know that the strain due to loading on adjacent teeth is a small effect. And we assume that the unmeasured strain reading on tooth 0 due to loading on tooth 1 is identical to the strains measured under similar conditions on tooth 1 due to a load applied on tooth 2. Likewise, when we calculate forces on tooth 2, we make a similar assumption that unmeasured readings from tooth 3 due to loading on tooth 2 are identical to measured readings on tooth 2 due to loading on tooth 1. Equation (4.4) thus becomes

$$
\begin{Bmatrix} F_{0n} \\ F_{0f} \\ F_{1n} \\ F_{1f} \\ F_{2n} \\ F_{2f} \end{Bmatrix} = \begin{bmatrix} a_{11} & \cdots & \cdots & \cdots & \cdots & a_{16} \\ \cdots & \cdots & \cdots & \cdots & \cdots & \cdots \\ \cdots & \cdots & \cdots & \cdots & \cdots & \cdots \\ \cdots & \cdots & \cdots & \cdots & \cdots & \cdots \\ \cdots & \cdots & \cdots & \cdots & \cdots & \cdots \\ a_{61} & \cdots & \cdots & \cdots & \cdots & a_{66} \end{bmatrix} \begin{Bmatrix} S_{0c} \\ S_{0t} \\ S_{1c} \\ S_{1t} \\ S_{2c} \\ S_{2t} \end{Bmatrix} \quad (A1)
$$

where $a_{ij}$ is a function of roll angle. Since there are only one or two teeth in contact at any one time, there are only two or four nonzero rows and columns in equation (A1), so the matrix is effectively only of order two or four. Any $a_{ij}$ corresponding to a tooth outside of the contact region is zero.

To illustrate the significance of the dominant terms in this matrix, for the purposes of this example only, cross-coupling terms[1] are disregarded. The normal force $F_{1n}$ simplifies to

$$ F_{1n} = a_{33}S_{1c} + a_{34}S_{1t} \quad (A2) $$

where $F_{1n}$ = normal force on tooth 1; $S_{1c}$ = compressive strain on tooth 1; and $S_{1t}$ = tensile strain on tooth 1.

The coefficients $a_{33}$ and $a_{34}$ are plotted in Fig. A1. It is notable that the tension gage has less influence on the computation of normal force than the compressive gage. Indeed, at a roll angle of 28° the coefficient $a_{34}$ becomes zero; the tensile gage then has no effect on $F_n$.

Similarly, the friction force (see Fig. A2) is described (again disregarding cross-coupling terms) by

$$ F_{1f} = a_{43}S_{1c} + a_{44}S_{1t} \quad (A3) $$

where $F_{1f}$ = normal force on tooth 1.

---

[1]Cross-coupling terms will assume a much greater significance in the case of thin-rim gears where the strain at a tooth fillet is significantly affected by the loading on an adjacent tooth.

To aid in the interpretation of these coefficients, it is useful to plot the tooth strain versus roll angle, for the tension and compressive gages. This is given in Fig. A3; the data shown here were obtained from taking the average of the calibration curves in Fig. 6.

The influence coefficients for the friction force show why accuracy is important. Recall that tensile and compressive outputs are similar in magnitude but opposite in sign; therefore the resultant value of friction is a small (approximately 10 percent) difference obtained from the products $a_{43}S_{1c}$ and $a_{44}S_{1t}$ in equation (A3).
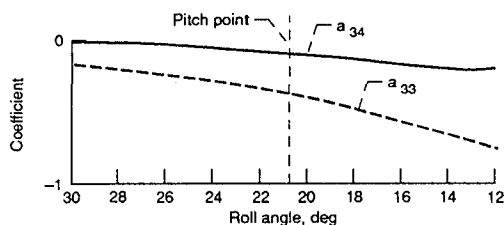


Figure A1.—Strain coefficients $a_{33}$ and $a_{34}$ for calculation of normal force (eq. (A2)).
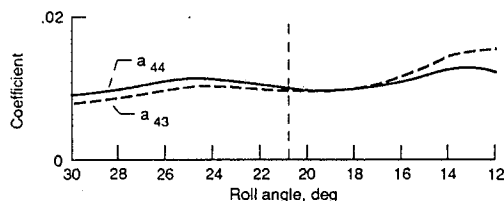


Figure A2.—Strain coefficients $a_{43}$ and $a_{44}$ for calculation of friction force (eq. (A3)).
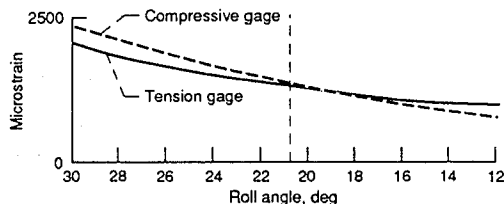


Figure A3.—Single tooth strain data obtained from Figure 6. (Tensile curve is average of two curves of Fig 6(a); compressive curve is average of two curves of Fig 6(b) and is shown as positive for comparison with tensile data.)

# 8. REFERENCES

1. Lin, H.H.; Huston, R.L.; and Coy, J.J.: On Dynamic Loads in Parallel Shaft Transmissions. 1: Modelling and Analysis. NASA TM-100180, 1987.

2. Lin, H.H.; Huston, R.L.; and Coy, J.J.: On Dynamic Loads in Parallel Shaft Transmissions. 2: Parameter Study. NASA TM-100181, 1987.

3. Benedict, G.H.; and Kelly, B.W.: Instantaneous Coefficients of Gear Tooth Friction. ASLE Trans., vol. 4, no. 1, 1961, pp. 59-70.

4. Anderson, N.E.; and Loewenthal, S.H: Spur-Gear-System Efficiency at Part and Full Load. NASA TP-1622, 1980.

5. Krantz, T.L.; and Handschuh, R.F.: Efficiency Study Comparing Two Helicopter Planetary Reduction Stages. AIAA Paper 90-2156, July 1990 (Also, NASA TM-103106, 1990).

6. Dowson, D.; and Higginson, G.R.: Elastohydrodynamic Lubrication, Pergamon, Oxford, 1966.

7. Dyson, A.: Frictional Traction and Lubricant Rheology in Elastohydrodynamic Lubrication. Philos. Trans., vol. A266, no. 1170, 1970, pp. 1-33.

8. Oswald, F.B., et al.: Comparison of Analysis and Experiment for Dynamics of Low Contact Ratio Spur Gears. NASA TM-103232, 1991.

9. Cornell, R.W.: Compliance and Stress Sensitivity of Spur Gear Teeth. ASME PAPER 80-C2/DET-24, Apr. 1981.

10. McFadden, P.D.: Examination of a Technique for the Early Detection of Failure in Gears by Signal Processing of the Time Domain Average of the Meshing Vibration. Mech. Syst. Signal Process., vol. 1, no. 2, 1987, pp. 173-183.

11. Drago, R.J.; and Pizzigati, G.A.: Some Progress in the Accurate Evaluation of Tooth Root and Fillet Stresses in Lightweight, Thin-Rimmed Gears. American Gear Manufacturers Association, Fall Technical Meeting, Washington, D.C. Oct. 1980. AGMA Paper 229.21.

| 1. Report No. NASA TM -103281 AVSCOM TR 90 - C - 023 | 2. Government Accession No. | 3. Recipient's Catalog No. |
|---|---|---|
| **4. Title and Subtitle** Dynamic Measurements of Gear Tooth Friction and Load | | **5. Report Date** |
| | | **6. Performing Organization Code** |
| **7. Author(s)** Brian Rebbechi, Fred B. Oswald, and Dennis P. Townsend | | **8. Performing Organization Report No.** E -6020 |
| | | **10. Work Unit No.** 505 – 63 – 36 1L162211A47A |
| **9. Performing Organization Name and Address** NASA Lewis Research Center Cleveland, Ohio 44135 - 3191 and Propulsion Directorate U.S. Army Aviation Systems Command Cleveland, Ohio 44135 - 3191 | | **11. Contract or Grant No.** |
| | | **13. Type of Report and Period Covered** Technical Memorandum |
| **12. Sponsoring Agency Name and Address** National Aeronautics and Space Administration Washington, D.C. 20546 - 0001 and U.S. Army Aviation Systems Command St. Louis, Mo. 63120 - 1798 | | **14. Sponsoring Agency Code** |

**15. Supplementary Notes**

**16. Abstract**

As part of a program to study fundamental mechanisms of gear noise, static and dynamic gear tooth strain measurements were made on the NASA gear-noise rig. Tooth-fillet strains from low-contact-ratio spur gears were recorded for 28 operating conditions. A method is introduced whereby strain gage measurements taken from both the tension and compression sides of a gear tooth can be transformed into the normal and frictional loads on the tooth. This technique was applied to both the static and dynamic strain data. The static case results showed close agreement with expected results. For the dynamic case, the normal-force computation produced very good results, but the friction results, although promising, were not as accurate. Tooth sliding friction strongly affected the signal from the strain gage on the tension side of the tooth. The compression gage was affected by friction to a much lesser degree. The potential of the method to measure friction force has been demonstrated, but further refinement will be required before this technique can be used to measure friction forces dynamically with an acceptable degree of accuracy.

| 17. Key Words (Suggested by Author(s)) Gears; Gearing; Dynamic load; Dynamic friction; Friction; Dynamics | 18. Distribution Statement Unclassified–Unlimited Subject Category 37 | | |
|---|---|---|---|
| **19. Security Classif. (of the report)** Unclassified | **20. Security Classif. (of this page)** Unclassified | **21. No. of pages** 14 | **22. Price\*** A03 |